

Article

Analysis of Buckling Deformation for the Side Plate of Rectangular CSFT Column Based on Plate Theory with Bi-Axial Loads

Bing Xu ^{1,*}, Lang Wang ^{1,2}, Chunyan Xiang ³ and Zhenyu Han ^{1,4}

¹ Civil Engineering Department, Yancheng Institute of Technology, Yancheng 224051, China; wl18905100097@163.com (L.W.); m18361651799@163.com (Z.H.)

² School of Civil Engineering and Architecture, Anhui University of Science and Technology, Huainan 232001, China

³ School of Civil Engineering and Architecture, Wuhan Institute of Technology, Wuhan 430074, China; xcy15827036006@163.com

⁴ School of Electric Power Engineering, Kunming University of Science and Technology, Kunming 650500, China

* Correspondence: bateren@126.com

Abstract: In this paper, under the condition of bidirectional stress, the buckling deformation of the side plate in a rectangular concrete-filled steel tube (CFST) column has been studied in detail. We have conducted a theoretical analysis, an experimental validation and a finite element simulation to investigate the influences of the height-width ratios and Nominal Poisson's ratios on the buckling form of the side plate, and we also try to explain the change of buckling form between unidirectional and bidirectional stress, both of them can provide a good reference and basis for design and application of the CFST column. The specific work can be summarized as follows: Firstly, a theoretical analysis has been conducted to study the buckling coefficient solution method of the thin plate under the conditions of axial compress and transverse tension. Then, under the conditions of the unidirectional and the bidirectional stress, a comparative study is carried out to investigate the changing relationship of the buckling coefficient (k) of the side plate; the results indicate that the buckling characteristic is changed due to the bidirectional stress, meanwhile, the buckling coefficient and the number of buckling half-wave will increase. Furthermore, the existing outcomes and the numerical simulations are adopted to study the relevance between the number of the elastic buckling half-wave in the side plate and the corresponding height-width ratio of the component; the results indicate that the former is larger than the latter. Finally, based on the obtained, the buckling relationship curve, the conclusion can be drawn as follows: when the bidirectional stress has been applied to the side plate, there is an equal interval between the different buckling half-waves; meanwhile, the interval shows a quadratic function reduce trend with the increase of nominal Poisson's ratio.

Keywords: rectangular concrete-filled steel tube column; elastic buckling; buckling coefficient



Citation: Xu, B.; Wang, L.; Xiang, C.; Han, Z. Analysis of Buckling Deformation for the Side Plate of Rectangular CSFT Column Based on Plate Theory with Bi-Axial Loads. *Buildings* **2022**, *12*, 626. <https://doi.org/10.3390/buildings12050626>

Academic Editors: Luca Pela and Fulvio Parisi

Received: 1 April 2022

Accepted: 5 May 2022

Published: 9 May 2022

Publisher's Note: MDPI stays neutral with regard to jurisdictional claims in published maps and institutional affiliations.



Copyright: © 2022 by the authors. Licensee MDPI, Basel, Switzerland. This article is an open access article distributed under the terms and conditions of the Creative Commons Attribution (CC BY) license (<https://creativecommons.org/licenses/by/4.0/>).

1. Introduction

In several decades, concrete-filled steel tube (CFST) components have been widely used due to the increasing construction of out-of-codes engineering and super high-rise buildings. This type of component illustrates a good bearing capacity because the steel tube can provide a forced constraint to the internal concrete and share the external loading with concrete together. However, when columns are damaged, although the cross-sections of each column are diverse, the buckling and voiding usually emerge in the steel tube [1–4]. Regarding this phenomenon, Yang et al. [5] conducted a quantified analysis to evaluate the influence of the voiding in the steel tube on the bearing capacity of CFST, and the result showed that the ultimate bearing capacity will be decreased by 20% when the sectional voiding rate of the test CFST exceeds 2%. Thus, from the perspective of guaranteeing

structural safety, it is more practical and valuable to study the voiding phenomenon between steel tubes and concrete.

The voiding usually has occurred in CFST due to the buckling in the outer plane of the steel tube. Based on the thin plate theory, the cause of the phenomenon can be analyzed and explained as follows: During the service period or the mechanical test loading process, the external deformation will emerge after the elastic buckling of the outer plane [6], then, the steel plate has a weak constraint on the core concrete; further, the yielded steel plate will cause a plastic deformation [7], which is the main reason for the voiding in CFST [8]. Regarding this problem, there are numerous studies which have been done. For example, Uy and Bradford [9] theoretically explained the elastic buckling problem of the steel plate in the steel-concrete composite structure using the finite strip analysis, and the computational method of the stable bearing capacity was proposed. Tao et al. [10] implemented a theoretical analysis on the elastic buckling problem of steel tube side plate under the axial load, then modified the equation of ultimate bearing capacity of side plate under the condition of uniaxial load and the width-thickness ratio of the plate in AS4100 [11]. Then, Liang et al. [12] experimentally evaluated the influences of the different width-thickness ratios of the plate on the bearing capability of the component; after that, the computational method of the steel tube bearing capability was proposed based on the width-thickness ratio. After that, Yang et al. [13] presents an analytical study of local buckling of steel plates in CFST columns. They get an approximate solution by Rayleigh–Ritz method, and it is in good agreement with the real local buckling stress of the steel plate. Long and Zeng [14] consider the influences of horizontal spacing and diameter of binding bars to propose a refined model, which is exploited to study the local buckling of rectangular CFST columns with binding bars under axial compression. Moreover, due to the high ambient temperature, the steel tube will be softened, and the axial stress will cause the buckling, further to threaten the bearing capacity of the structure. Lyu et al. [15] conduct a comparative study to find out the axial compressive performance of six thin-walled CFST square column specimens with steel bar stiffeners and two non-stiffened specimens in the different temperature conditions. Kamil et al. [16] aim to the local and post-local buckling of steel tube in the specific temperature condition, where a numerical research has been used to explain the local buckling effects on the responses of rectangular thin-walled CFST columns under the temperature influence.

Although it is a good guideline for the practical engineering design and application to refer to the elastic bearing capability analysis of the plate under the condition of uniaxial load, when the transverse deformation has occurred in the internal concrete, the steel tube will enhance the bearing capability by applying the constraints. Meanwhile, due to the reaction force, the concrete will cause the transverse deformation of the steel tube as well; namely, the transverse stress also exists in the tube, which may cause the buckling further. The study of Song et al. [17] pointed out that the buckling will transform the state of axial compression into the transverse tension, which will influence the buckling form.

An important reason why the steel tube and concrete can work together is that coefficients of linear expansion of two materials are close. Furthermore, in the early loading stage, the deformations of two materials are approximately equal. At the same time, referring to the existing specifications and codes [11,18,19], the ultimate bearing capacity of the rectangular CFST can be considered as a combination of the bearing capabilities of the concrete and the steel tube; namely, on the prerequisite of deformation coordination, it can be considered as each part undertakes the external load independently until the ultimate state has been achieved.

Regarding the abovementioned statement and assumption, the adhesion effort between the steel tube and concrete is also ignored. In this paper, based on thin-plate stability theory, aiming at the rectangular CFST under the bidirectional stress, the elastic buckling behavior in the side plate will be investigated and studied. We consider the different influences of height-width ratios and Nominal Poisson's ratios to numbers of buckling half-wave, and the experiments and finite element simulations are both used to verify the

analytical results. The results and findings are of great significance to the study, design and application of the similar and/or same component in the practical engineering application.

The remaining sections are organized as follows: Section 2 has introduced the theoretical analysis of the buckling in the side plate of steel tube in CFST. Section 3 introduces experimental research on the buckling characteristics. Then, Section 4 utilizes finite element method to investigate and verify the development of the buckling. After that, Section 5 has discussed the influence of the height-width ratio on the buckling. Finally, we draw several conclusions and outlooks in Section 6.

2. Buckling Theory Analysis of the Side Plate of the Rectangular Steel Tube

During the service period or loading process, the steel tube will be squeezed due to the deformation of concrete, causing the transverse stress in the tube. Regarding this condition, the stress state of the side plate is transformed into bidirectional stress (axial compression and transverse tension) from unidirectional stress (axial compression) (Figure 1). However, as the boundary condition of the component has not changed, the strength and stability of the side plate will be varied with the stress state.

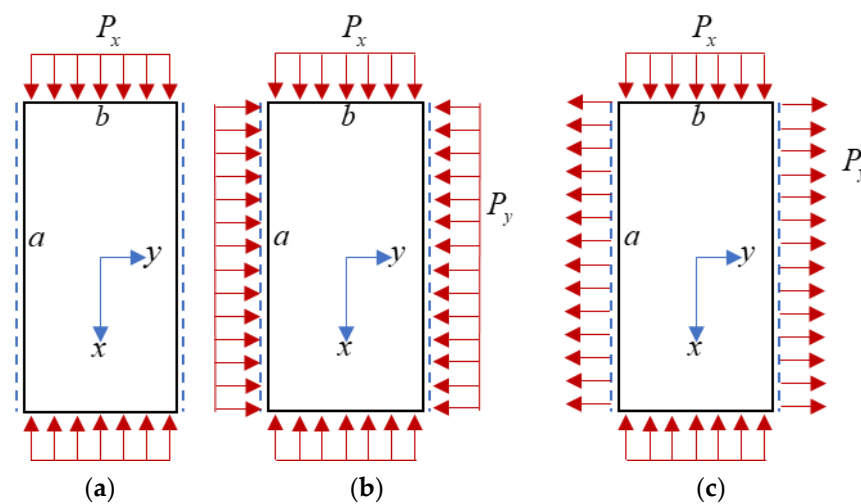


Figure 1. Stress form of buckling of the side plate. (a) Axial compression. (b) Axial compression and transverse compression. (c) Axial compression and transverse tension.

2.1. Elastic Buckling Behavior of the Side Plate of the Steel Tube under Unidirectional Load

For the state of the unidirectional loading, the stress has shown uniform distribution in the cross-section of the steel tube, and the corner only provides simply supported constraints. Regarding the one side of the rectangular steel tube, the constraint of the plate can be assumed as simply supported. Then, assuming that the longitudinal uniform loading P_x has been applied to the surface, the corresponding deflection can be calculated as follows:

$$w = \sum_{m=1}^{\infty} \sum_{n=1}^{\infty} A_{mn} \sin \frac{m\pi x}{a} \sin \frac{n\pi y}{b} \quad (1)$$

where w is the deflection of the plate in the point of (x, y) ; A_{mn} means the maximum out-of-plane deformation of the half-wave of buckling; m and n are the numbers of the buckling half-wave in the direction of x and y , respectively; a and b stand for the height and width of the plate, respectively. In this paper, n can be defined as 1 and m is influenced by the height-width ratio of the plate, namely, a/b .

Then the relationship of the load-deformation in the plate can be expressed as follows:

$$D\nabla^4 w + P_x \frac{\partial^2 w}{\partial x^2} = 0 \quad (2)$$

where $D = \frac{Et^3}{12(1-\mu^2)}$ is the bending stiffness of a thin plate; then to substitute Equation (1), the differential equation can be rewritten as follows:

$$\sum_{m=1}^{\infty} \sum_{n=1}^{\infty} A_{mn} [D(\frac{m^2}{a^2} + \frac{n^2}{b^2})^2 - P_x \frac{m^2}{\pi^2 a^2}] \sin \frac{m\pi x}{a} \sin \frac{n\pi y}{b} = 0 \quad (3)$$

According to Equation (3), when P_x has been defined as a small value, namely, the axial load has been applied to the plate, thus, only the in-plane compression deformation has occurred, and $A_{mn} = 0$. While with the increase of P_x , the plate is unstable and begins to deform, for this situation, to satisfy Equation (3) and $A_{mn} \neq 0$, we can deduce the following equation:

$$D(\frac{m^2}{a^2} + \frac{n^2}{b^2})^2 - P_x \frac{m^2}{\pi^2 a^2} = 0 \quad (4)$$

Considering this specific situation, the corresponding external load can be expressed as follows:

$$P_x = \frac{\pi^2 a^2 D}{m^2} (\frac{m^2}{a^2} + \frac{n^2}{b^2})^2 = \frac{\pi^2 D}{b^2} (\frac{mb}{a} + \frac{1}{\frac{mb}{a}})^2 \quad (5)$$

Let

$$k = (\frac{mb}{a} + \frac{1}{\frac{mb}{a}})^2 \quad (6)$$

and substitute it into Equation (5). Thus, Equation (5) can be simplified as the standard formula of stability bearing capacity in AS4100 [11]. Then, according to Equation (6), as shown in Figure 2, the change curve can be obtained.

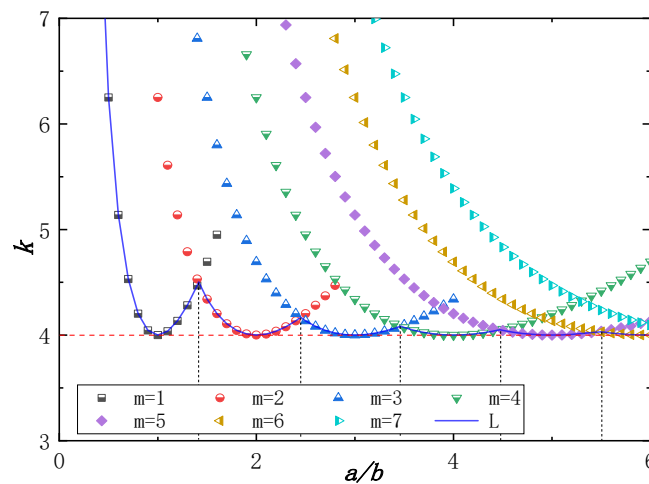


Figure 2. The variation of the buckling coefficient of the side plate with different height-width ratios and half-wave numbers in the direction of x (unidirectional stress).

As shown in Figure 2, for the plate under the unidirectional stress, the envelope curve indicates that the number of buckling half-wave (m) and the height-width ratio of the plate (a/b) have synergistic effects on the buckling coefficient (k). Meanwhile, with the increase of a/b and m , the buckling coefficient (k) gradually decreases and then infinitely closes to 4.

2.2. Elastic Buckling Behavior of the Side Plate of the Steel Tube under Bidirectional Load

When the steel tube is squeezed due to the deformation of the internal concrete, the transverse stress has gradually emerged in the side plate, meanwhile, the stress state of the side plate is transformed into bidirectional stress from unidirectional stress. Assuming that the transverse loading in the plate is P_y , the longitudinal uniform loading keep P_x

(as shown in Figure 1c), then the relationship of the load-deformation in the plate can be expressed as follows:

$$D\nabla^4 w + P_x \frac{\partial^2 w}{\partial x^2} + P_y \frac{\partial^2 w}{\partial y^2} = 0 \quad (7)$$

then to substitute Equation (1), the differential equation can be rewritten as follows:

$$\sum_{m=1}^{\infty} \sum_{n=1}^{\infty} A_{mn} \left[D \left(\frac{m^2}{a^2} + \frac{n^2}{b^2} \right)^2 - P_x \frac{m^2}{\pi^2 a^2} - P_y \frac{n^2}{\pi^2 b^2} \right] \sin \frac{m\pi x}{a} \sin \frac{n\pi y}{b} = 0 \quad (8)$$

Since there is already a deflection in the plate in this case, to satisfy the Equation (8) and $A_{mn} \neq 0$, we can deduce the following equation:

$$D\nabla^4 w + P_x \frac{\partial^2 w}{\partial x^2} + P_y \frac{\partial^2 w}{\partial y^2} = 0 \quad (9)$$

Assuming that the constraints generated by the steel tube have been applied to the component, the nominal Poisson's ratio of rectangular CSFT can be represented as μ' , thus, we can obtain the following equation:

$$\varepsilon_y = -\mu' \varepsilon_x \quad (10)$$

Then the nominal transverse stress of the steel tube can be calculated as follows:

$$\sigma_y = E_s \varepsilon_y = -E_s \mu' \varepsilon_x = -\mu' \sigma_x \quad (11)$$

where ε_y and ε_x are the nominal transverse and longitudinal strains, respectively; σ_x represents the nominal longitudinal stress. Furthermore, the relationship between P_x and P_y can be described as follows:

$$P_y = \sigma_y t = -\mu' \sigma_x t = -\mu' P_x \quad (12)$$

To substitute Equation (12) to Equation (9), for the state of the bidirectional loading, the buckling bearing capacity calculation formula of the side plate can be rewritten as follows:

$$P_x = \frac{\pi^2 D}{a^2} \frac{(m^2 + n^2 \frac{a^2}{b^2})^2}{m^2 - \mu' n^2 \frac{a^2}{b^2}} = \frac{\pi^2 D}{b^2} \frac{(m^2 \frac{b}{a} + n^2 \frac{a}{b})^2}{m^2 - \mu' n^2 \frac{a^2}{b^2}} \quad (13)$$

Let

$$k = \frac{(m^2 \frac{b}{a} + n^2 \frac{a}{b})^2}{m^2 - \mu' n^2 \frac{a^2}{b^2}} \quad (14)$$

Then we can obtain the calculation formula of the buckling coefficient for the plate under the bidirectional stress. Meanwhile, according to Equation (14), for the plate under the bidirectional stress, not only the number of buckling half-wave (m) and the height-width ratio of the plate (a/b), but also the nominal Poisson's ratio (μ') can make an effort on the buckling coefficient (k). The experiment of Li et al. [20] also reported the nominal Poisson's ratio gradually rises from 0.264 to 0.5 with the increase of external loading, and then keeps a constant value. Figure 3 illustrates the change curve of the buckling coefficient (k) which varies with the nominal Poisson's ratio (μ'). It can be seen from Figure 3 that when the height-width ratio of the plate (a/b) is fixed, the number of buckling half-wave (m) will increase with the rising of the nominal Poisson's ratio (μ'), further to enhance the corresponding maximum in the buckling coefficient curve (Figure 4). Compared to the state of the unidirectional loading, the transverse stress makes the buckling coefficient of the plate with the same size increase. Meanwhile, when the height-width ratios of the two

plates (a/b) are consistent, the corresponding number of buckling half-wave has also risen with the increase of the nominal Poisson ratio (μ').

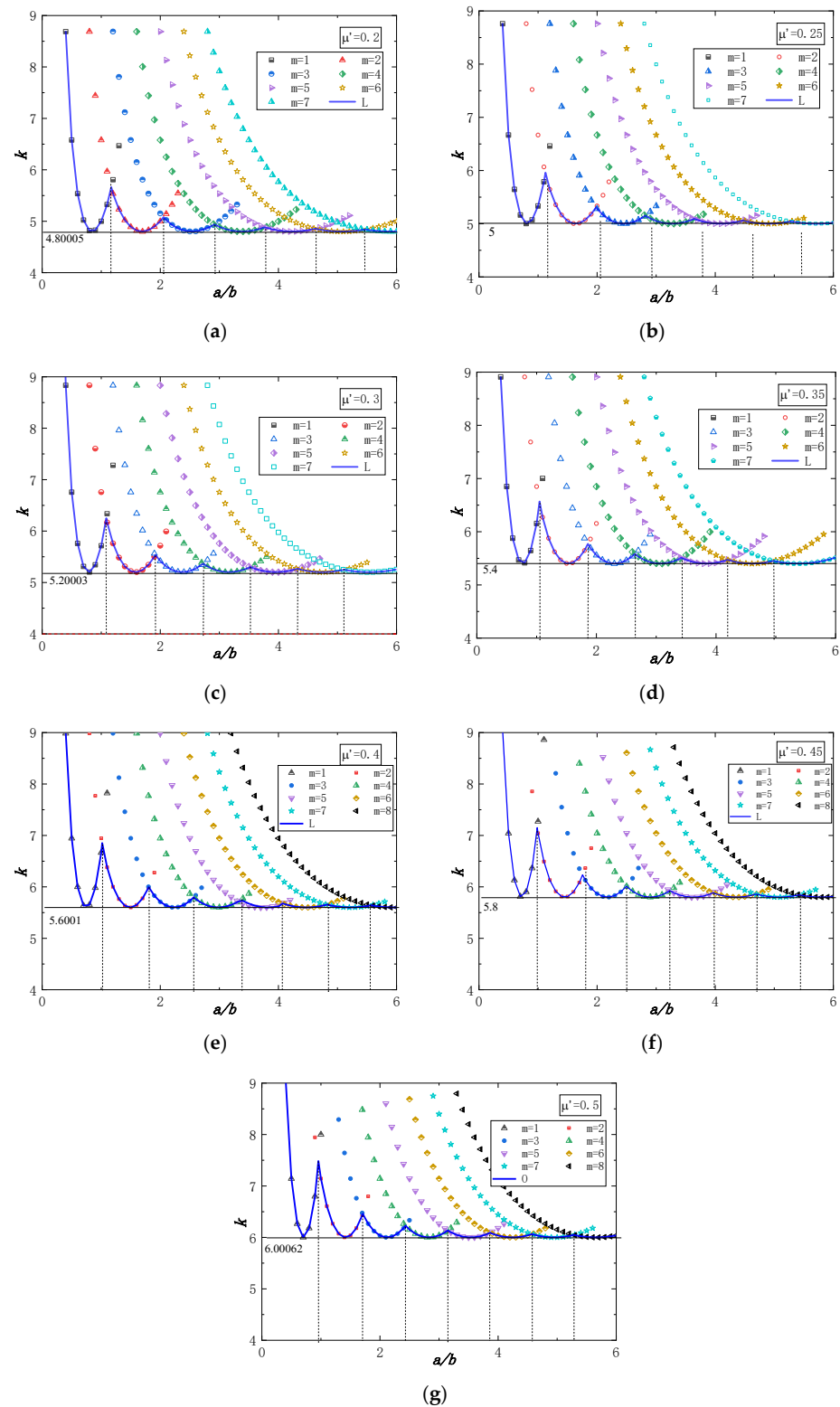


Figure 3. (a–g) The variation of the buckling coefficient of the side plate with different height width ratios, half-wave numbers, and nominal Poisson’s ratios (bidirectional stress).

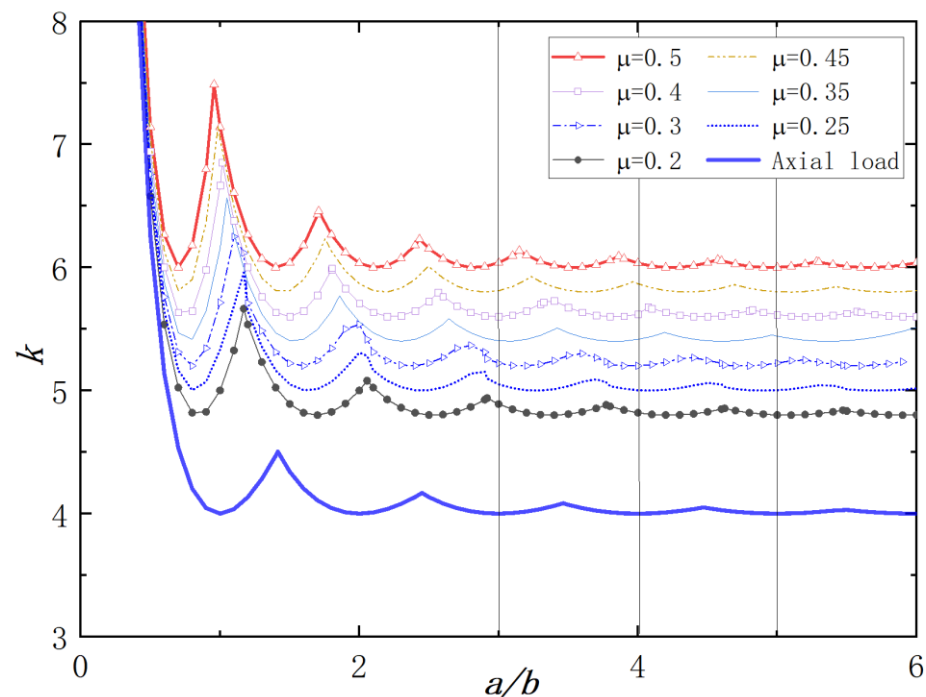


Figure 4. The variation of the buckling coefficient of the side plate with different nominal Poisson's ratios (bidirectional stress).

3. Buckling Characteristics of the Side Plate of the Steel Tube in Rectangular CSFT

3.1. Buckling Phenomenon of the Side Plate of the Steel Tube in Rectangular CSFT under the Axial Compression

In the studies of Refs. [20–23], we can find that the unrecoverable buckling appeared in the side plate as the damage has occurred in the component. Meanwhile, as shown in the figures of buckling forms, except for the component of UCFT3-2, the numbers of buckling half-wave (m) all exceed the designed height-width ratio of the side plate (Table 1). Based on the elastic buckling theory of the plate in the unidirectional loading, the value of the buckling half-wave number is equal to the designed height-width ratio, but the observed buckling half-wave numbers are all larger than the designed height-width ratio, which verifies that the number of the buckling half-wave is larger than the designed height-width ratio when the dimensional size is fixed, and the loading has increased.

Table 1. Buckling characteristics of the side plate in rectangular CSTC under axial compression in existing studies (unit: mm).

Item	Number	Width (b)	Thickness (t)	Height (a)	Number of Half-Wave (m)
Figure 5a	CUS28 [21]	280	2.5	840	4
Figure 5b	SCA-30-2 [22]	900	4	300	4
Figure 5c	UCFT3-2 [20]	250	2.5	750	2
Figure 5d	t2c2-316 [23]	202.64	4.62 + 1.32	600	4
Figure 5e	t1c2-316 [23]	201.68	4.14 + 0.84	600	5
Figure 5f	t3c2-316 [23]	203.76	5.18 + 1.88	600	4

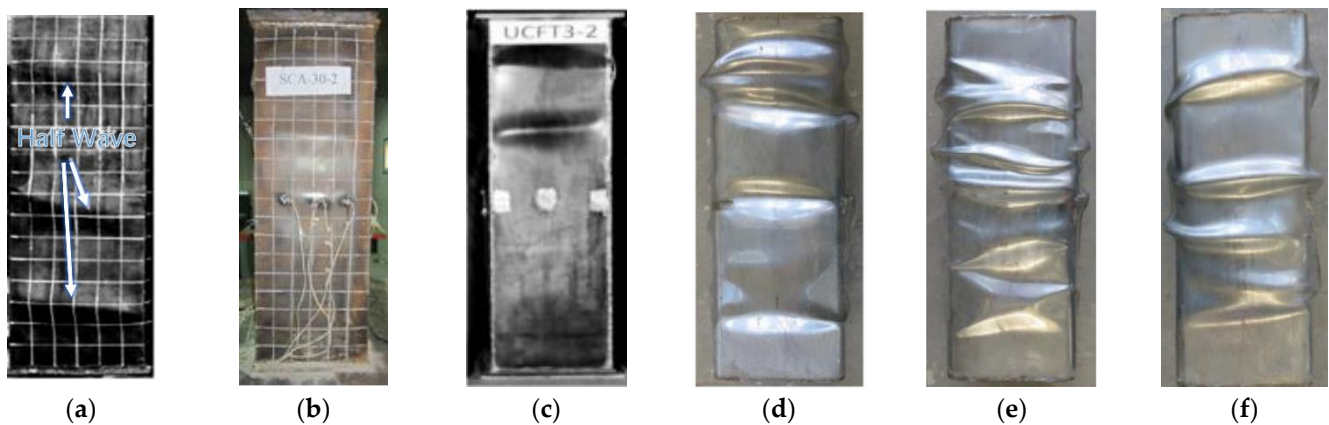


Figure 5. The buckling forms of the side plate of the steel tube in rectangular CSFT in existing studies.

3.2. The Axial Compression Experiment of Rectangular CSFT Short Column

To compare and research the relationship between the buckling half-wave and loading, we have designed a rectangular CSFT short column with $300 \times 300 \times 900$ mm, and the thickness of the steel tube is 4 mm, then the axial compression test has been conducted. The experimental results can be plotted in Figure 6. During the process of the experiment, in the early stage, there is no obvious deformation which occurred in the component, the nominal Poisson's ratio shows linear change with the increasing loading (Figure 6b). Then, when the experimental loading has achieved about 60% of the ultimate bearing capacity, the longitudinal strain will decrease, the turning point has occurred in the curve, the turning phenomenon can be owed to the elastic deformation of the plate, namely, the elastic buckling has emerged in the plate. After that, when the experimental loading has achieved about 80% of the ultimate bearing capacity, it is obvious that the buckling has occurred in the surface at the concentrated position of the slip line, and the stress-strain curves of different sides show a bifurcation phenomenon (Figure 6c,d), where the turning point has occurred in the nominal strain curve (Figure 6b). This situation is caused by the dislocated buckling in the side plate; meanwhile, the buckling half-wave in the surface shows a growth trend with the increasing loading, as well as the more obvious buckling phenomenon.

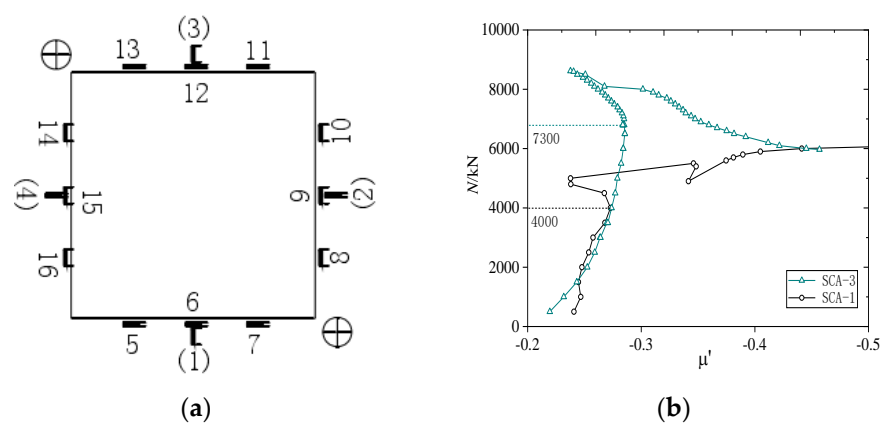


Figure 6. Cont.

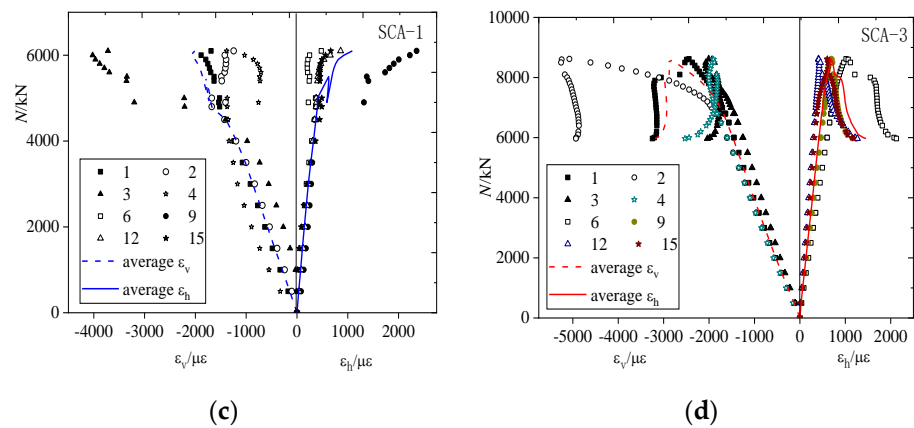


Figure 6. The stress of analysis of the rectangular CSFT short column. (a) Measuring point. (b) Load-Nominal Poisson’s ratio curve. (c) Load-strain curve of SCA-1. (d) Load-strain curve of SCA-2.

4. Finite Element Verification of Elastic Buckling Development of the Side Plate of the Steel Tube in Rectangular CSFT Short Column

To investigate the buckling behavior of steel tubes in detail, in this section, ABAQUS [3,24] is utilized to simulate the components. Three rectangular CSFT short column models with different height-width ratios (3:1, 4:1, and 5:1 [25]) have been simulated, and then, under the condition of axial loading, we analyzed the changing relationship of buckling deformation in the surface of the side plate. For the internal concrete, the material property of C30 concrete and the concrete damage plastic constitutive model are adopted; the steel is Q345 steel with the bilinear elastic-plastic constitutive model. Other parameters for the analysis can be referred to Ref. [15]. Thus, the element of the concrete adopts the eight-node three-dimensional solid Unit C3D8. The outer steel tube adopts the shell thermal analysis Unit S4R. The contact type among the steel tube and core concrete is set to tangential behavior, and the friction coefficient is 0.3. The buckling behavior of the side plate of the steel tube has been illustrated in Figure 7.

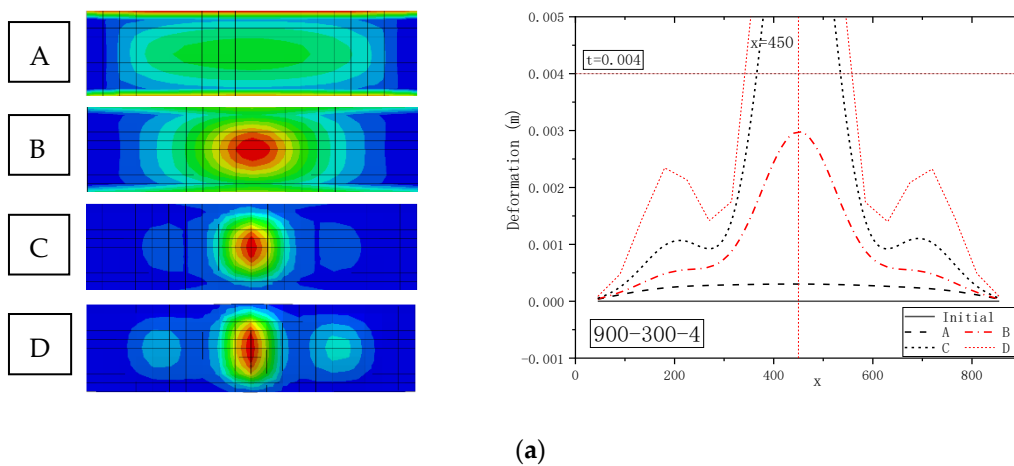


Figure 7. Cont.

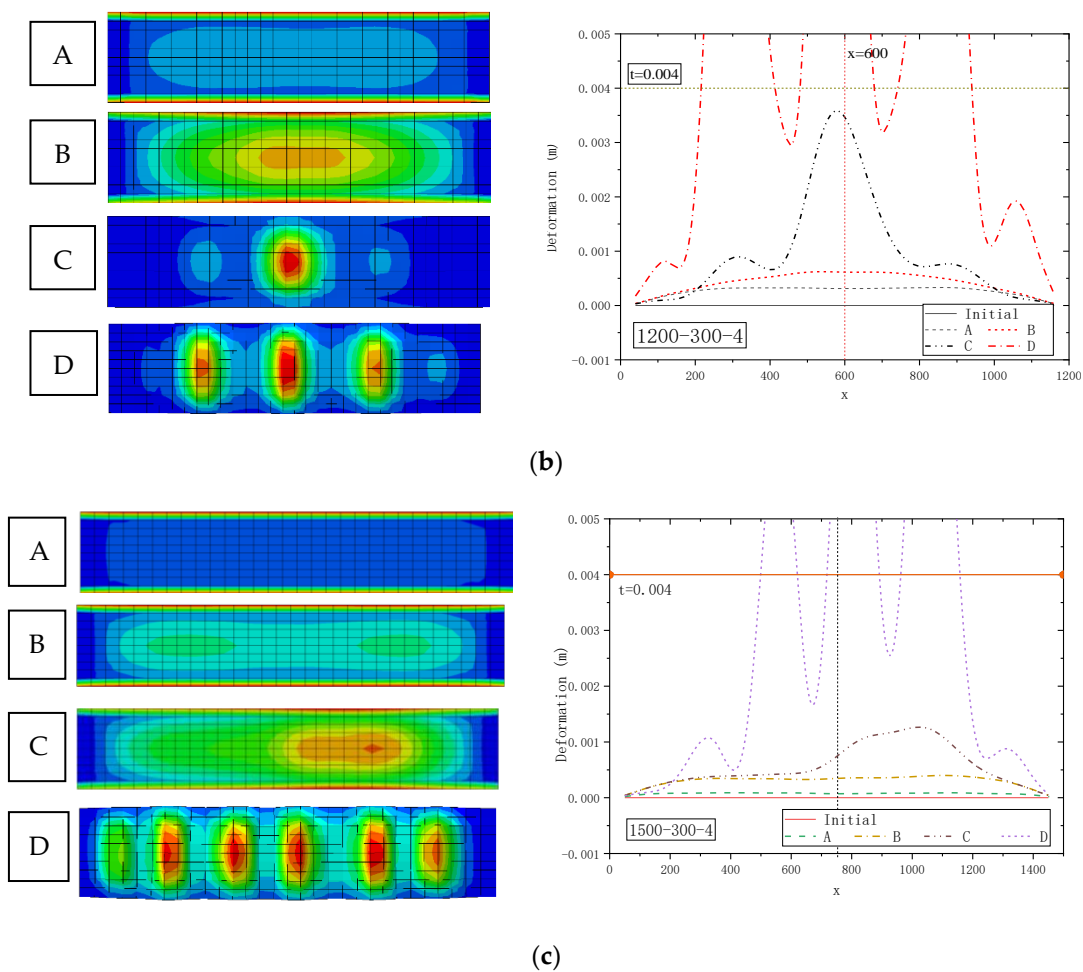


Figure 7. Buckling deformation forms of the side plate under different height-width ratios (A–C are the change of buckling deformation in the loading process, D is the final form). (a) $300 \times 300 \times 900$, $t = 4$. (b) $300 \times 300 \times 1200$, $t = 4$. (c) $300 \times 300 \times 1500$, $t = 4$.

As shown in Figure 7, for several different steel tubes with diverse height-width ratios, in final, the corresponding buckling numbers all exceed their height-width ratios. Meanwhile, from the results of three components, all of them observation showed the changes of the buckling form. For three components, the phenomenon has occurred between the form B and C (3:1), form A, B, and C (4:1), and form A, B, and C (5:1), respectively, which means the bidirectional stress has occurred in the plate due to the squeezing effect of the internal concrete, then to change the buckling form obviously with the change of stress state. The right of Figure 7 illustrates the buckling deformation in the different moments, according to the order of forms A, B, and C, it can be observed that the deformation of the latter is always a sudden change based on the former. The form of the sudden change shows growth in the number of the buckling half-wave, the distribution tends to be uniform, and the wavelength is shortened. The sudden change can be owed to the bidirectional stress that has occurred in the plate due to the squeezing effect of the internal concrete; in this situation, the number of buckling half-wave is more than the situation of the unidirectional stress. These phenomena also validate a principle, namely, for the fixed height-width ratio, the higher Poisson's ratio, the more buckling half-wave shown in the curve of the buckling coefficient. Moreover, with the increase of the buckling number, the peak value of the buckling deformation will decrease.

5. Discussion

The intersection points of the adjacent m -curve (Figures 3 and 4) are picked and listed in Table 2, and then to obtain the linear fitting of data (Figure 8). As shown in Table 2 and Figure 8, the following conclusion can be summarized: When the value of m has risen, the corresponding slope of a/b remains unchanged, which means for the same condition, the value of a/b is the main factor to influence the number of buckling half-wave. It can be summarized that when the value of b keeps unchanged, the more larger a , the more larger m . In addition, the equidistant growth trend also verifies that the wavelengths of elastic buckling half-waves in the plate should be equal, namely, the wavelengths are all equal to the interval.

Table 2. Height-width ratios of the plate corresponding to different numbers of buckling half-wave.

	$m = 1$	$m = 2$	$m = 3$	$m = 4$	$m = 5$	$m = 6$	$m = 7$
Unidirectional Stress	1.415	2.45	3.464	4.473	5.477	-	-
Bidirectional Stress	$\mu = 0.2$	1.170	2.056	2.918	3.772	4.627	5.472
	$\mu = 0.25$	1.126	1.984	2.817	3.642	4.465	5.285
	$\mu = 0.3$	1.086	1.918	2.725	3.525	4.322	5.117
	$\mu = 0.35$	1.049	1.858	2.642	3.419	4.192	4.963
	$\mu = 0.4$	1.016	1.804	2.566	3.321	4.073	4.822
	$\mu = 0.45$	0.987	1.753	2.497	3.232	3.963	4.693
	$\mu = 0.5$	0.957	1.708	2.432	3.149	3.862	4.573

NOTE: “-” means the values of a/b for the intersection point in Figure 3 overlaps.

Figure 8 has shown the linear fittings of height-width ratio and buckling half-wave number, which indicates a near growth. Then, under the condition of bidirectional stress, the slopes of fitting lines are collected and plotted in Figure 9 with the nominal Poisson’s ratio as X -axis. From Figure 9, it can be seen that: the slope of the fitting line has reduced with increasing relative Poisson’s ratio of the component, and it also shows a characteristic of the quadratic function. Thus, the nominal Poisson’s ratio also can be determined as a key parameter to the number of buckling half-wave, namely, the larger nominal Poisson’s ratio, the higher tensile stress in the side of the steel tube, then the more buckling half-waves, and the corresponding wavelength of half-wave is smaller.

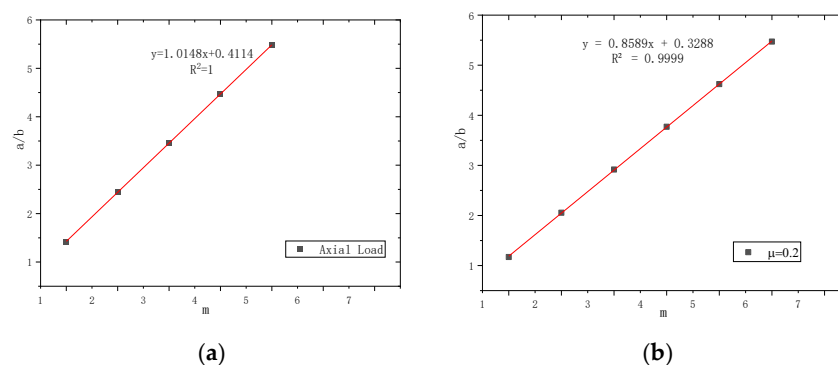


Figure 8. Cont.

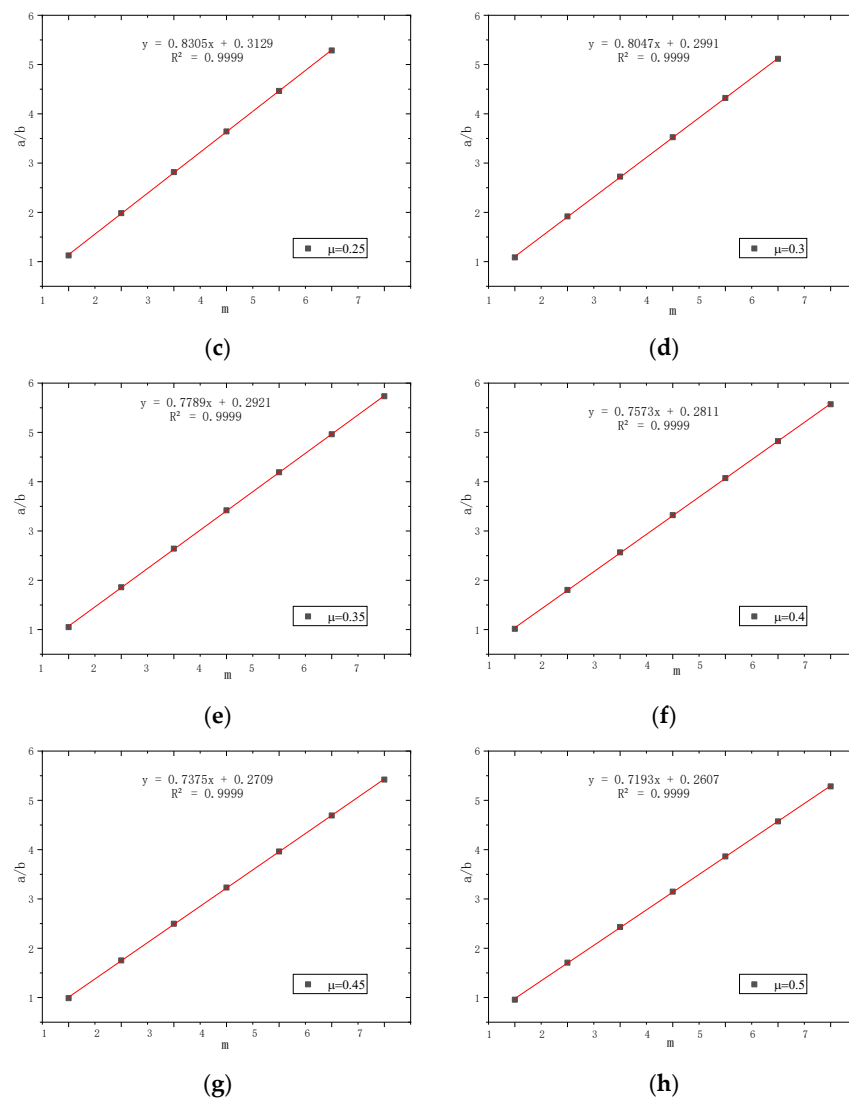


Figure 8. (a–h) The relationship between m and $\frac{a}{b}$.

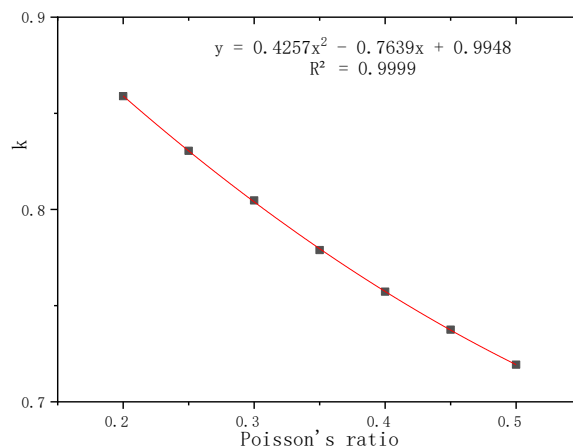


Figure 9. Relationship between the slope of the fitting curve and the Nominal Poisson's ratio.

6. Conclusions and Outlook

The buckling is the classical crack form of the rectangular CSFT short column, and the study of the buckling is of great significance to the structural failure characteristics and behavior. In this paper, first of all, we have conducted a theoretical analysis to research the

buckling of the side plate in the rectangular CSFT short column. Then, the experimental analysis and finite element verification are used to investigate the elastic buckling and its development characteristic of the steel tube under the loading process. Several conclusions can be summarized as follows:

- (1) For the condition of bidirectional stress, the buckling coefficient of the side plate is larger than the coefficient under the unidirectional stress, the corresponding value of m will increase. It can be explained that under the state of bidirectional stress when the buckling has occurred in the plate, the external loading and the number of buckling half-wave are both larger than the corresponding values under the condition of a unidirectional stress.
- (2) For the condition of longitudinal loading, when the failure has emerged in the side steel tube of the rectangular CSFT column, the number of buckling half-wave is larger than the height-width ratio (a/b) of the plate.
- (3) During the process of loading, for the side plate of the steel tube, the buckling form change can be owed to the stress state change of the component (from unidirectional stress to bidirectional stress). Meanwhile, with the increase of the transverse stress, the wavelength of the buckling half-wave will reduce while the number of buckling will rise.
- (4) For the same loading condition, in the intersection points of m -curve in the buckling coefficient curve, the interval between, adjacent of the height-width ratio (a/b) is fixed, and for the condition of bidirectional stress, the interval will decrease with the increasing Poisson's ratio.

For future work, there are some outlooks which are listed as follows:

- (1) Although the analytical study and experimental validation have been conducted in this paper, we only consider the failure of rectangular CSFT column under the condition of the bidirectional stress; some other factors, such as high ambient temperature, horizontal spacing and diameter of binding bars, etc., should be also investigated.
- (2) Several specimens are used to verify the theoretical results, which can reflect the main forming of the buckling deformation; in the future, we are going to design more test specimens to obtain a more accurate result for the needs of practical applications.

Author Contributions: Conceptualization, B.X.; methodology, C.X.; validation, C.X.; resources, B.X.; data curation, Z.H.; writing—original draft preparation, L.W.; writing—review and editing, B.X.; supervision, B.X.; project administration, B.X.; funding acquisition, B.X. All authors have read and agreed to the published version of the manuscript.

Funding: This research was funded by the Fundamental Research Funds for the Central Universities, CHD [300102212525].

Institutional Review Board Statement: Not applicable.

Informed Consent Statement: Not applicable.

Data Availability Statement: Not applicable.

Conflicts of Interest: The authors declare no conflict of interest.

References

1. Xiang, K.; Pan, Y.; Wang, G. Axial compression analysis of square concrete-encased concrete filled steel tubular stub columns after fire exposure. *Procedia Eng.* **2018**, *211*, 1151–1159. [[CrossRef](#)]
2. Cai, J.; He, Z.Q. Axial load behavior of square CFT stub column with binding bars. *J. Constr. Steel Res.* **2006**, *62*, 472–483. [[CrossRef](#)]
3. Ding, F.; Lu, D.; Bai, Y.; Zhou, Q.-S.; Ni, M.; Yu, Z.-W.; Jiang, G.-S. Comparative study of square stirrup-confined concrete-filled steel tubular stub columns under axial loading. *Thin Walled Struct.* **2016**, *98*, 443–453. [[CrossRef](#)]
4. Han, L.H.; Li, W.; Bjorhovde, R. Developments and advanced applications of concrete-filled steel tubular (CFST) structures: Members. *J. Constr. Steel Res.* **2014**, *100*, 211–228. [[CrossRef](#)]
5. Yang, S.C.; Wang, F.M.; Qu, P. Brief Introduction to the Core Concrete's Empty Influence on the Mechanical Performance of Concrete Filled Steel Tube Components. *J. Chongqing Jiaotong Univ. Nat. Sci.* **2008**, *27*, 360–365. (In Chinese)

6. Shahwan, K.W.; Waas, A.M. A mechanical model for the buckling of unilaterally constrained rectangular plates. *Int. J. Solids Struct.* **1994**, *31*, 75–87. [[CrossRef](#)]
7. Tao, Z.; Uy, B.; Liao, F.Y.; Han, L.H. Nonlinear analysis of concrete-filled square stainless steel stub columns under axial compression. *J. Constr. Steel Res.* **2011**, *67*, 1719–1732. [[CrossRef](#)]
8. Zhou, X.H.; Liu, Y.J.; Lei, J.; Ning, Z. Review on Mechanical Behavior Research of Concrete Filled Rectangular Hollow Section Tube Stiffened with PBL. *China J. Highw. Transp.* **2017**, *30*, 45–62. (In Chinese)
9. Uy, B.; Bradford, M.A. Elastic local buckling of steel plates in composite steel-concrete members. *Eng. Struct.* **1996**, *18*, 193–200. [[CrossRef](#)]
10. Tao, Z.; Uy, B.; Han, L.; Wang, Z.-B. Analysis and design of concrete-filled stiffened thin-walled steel tubular columns under axial compression. *Thin Walled Struct.* **2009**, *47*, 1544–1556. [[CrossRef](#)]
11. Standards Association of Australia. *Australian Standard AS4100; Steel Structures*. Standards Association of Australia: Sydney, Australia, 1998.
12. Liang, Q.Q.; Uy, B.; Liew, J. Nonlinear analysis of concrete-filled thin-walled steel box columns with local buckling effects. *J. Constr. Steel Res.* **2006**, *62*, 581–591. [[CrossRef](#)]
13. Yang, Z.Y.; Qiao, Q.Y.; Cao, W.L.; Gao, X. Axial compressive behavior of square steel tube confined rubberized concrete stub columns. *J. Build. Eng.* **2022**, *52*, 104371.
14. Long, Y.L.; Zeng, L. A refined model for local buckling of rectangular CFST columns with binding bars. *Thin-Walled Struct.* **2018**, *132*, 431–441. [[CrossRef](#)]
15. Lyu, X.; Xu, Y.; Xu, Q.; Yu, Y. Axial compression performance of square thin walled concrete-Filled steel tube stub columns with reinforcement stiffener under constant high-Temperature. *Materials* **2019**, *12*, 1098. [[CrossRef](#)]
16. Kamil, G.M.; Liang, Q.Q.; Hadi, M.N.S. Local buckling of steel plates in concrete-filled steel tubular columns at elevated temperatures. *Eng. Struct.* **2018**, *168*, 108–118. [[CrossRef](#)]
17. Song, Y.; Wang, R.; Li, J. Local and post-local buckling behavior of welded steel shapes in partially encased composite columns. *Thin Walled Struct.* **2016**, *108*, 93–108. [[CrossRef](#)]
18. ACI (American Concrete Institute). *Building Code Requirements for Structural Concrete and Commentary*; American Concrete Institute: Farmington Hills, MI, USA, 2011.
19. BSI (British Standards Institution). *Steel, Concrete and Composite Bridges—Part 4: Code of Practice for Design of Concrete Bridges. BS5400*; British Standards Institutions: London, UK, 2005.
20. Li, B.; Guo, S.Z.; Gao, C.Y. Experimental research on mechanical behavior of concrete filled thin-walled stiffened square steel tubular short column under axial load. *J. Build. Struct.* **2017**, *38*, 218–225. (In Chinese)
21. Huang, H.; Chen, M.C.; Wan, C.Y. Behavior of concrete-filled stiffened square steel tubes subjected to eccentric compressive load. *China Civ. Eng. J.* **2011**, *44*, 26–34. (In Chinese)
22. Zhang, J.G. *Research on the Mechanical Performance of Concrete-Filled Square Steel Tube Stiffened with PBL under Axial Compression Load*; Chang'an University: Xi'an, China, 2012. (In Chinese)
23. Ye, Y.; Zhang, S.; Han, L.; Liu, Y. Square concrete-filled stainless steel/carbon steel bimetallic tubular stub columns under axial compression. *J. Constr. Steel Res.* **2018**, *146*, 49–62. [[CrossRef](#)]
24. Chang, X.; Ru, Z.L.; Zhou, W.; Zhang, Y.-B. Study on concrete-filled stainless steel–carbon steel tubular (CFST) stub columns under compression. *Thin Walled Struct.* **2013**, *63*, 125–133. [[CrossRef](#)]
25. Tao, Z.; Wang, Z.B.; Yu, Q. Finite element modelling of concrete-filled steel stub columns under axial compression. *J. Constr. Steel Res.* **2013**, *89*, 121–131. [[CrossRef](#)]